

Transitional and permanent regimes in the adiabatic Floquet approach to photodissociation processes

Georges Jolicard¹, John P Killingbeck^{1,2}, David Viennot¹,
Jeanna Buldyreva³ and Pierre Joubert³

¹ Institut Utinam, UMR CNRS 6213, Université de Franche-Comté, Observatoire de Besançon, 41 bis avenue de l'Observatoire, BP1615, 25010 Besançon cedex, France

² Mathematics Centre, University of Hull, Hull HU6 7RX, UK

³ Institut Utinam, UMR CNRS 6213, Université de Franche-Comté, 16 route de Gray, 25000 Besançon Cedex, France

Received 24 September 2007, in final form 28 January 2008

Published 19 February 2008

Online at stacks.iop.org/JPhysA/41/095303

Abstract

Adiabatic formalisms are widely used, within the context of Floquet theory, to study photoreactive processes and control processes involving laser fields. In numerous cases, however, the use of the adiabatic hypothesis seems to be rendered problematic by the presence of one or more sudden variations in the chosen adiabatic parameters. The present paper shows that in such cases the behaviour of the system can be described quite accurately by using successive groups of a few instantaneous Floquet eigenvectors which are connected to each other by non-adiabatic transition factors. In the optical potential approach the relevant Floquet eigenvectors are those issuing from some bound states or from discretized states of vibrational continua. The approach described here leads to fast integration techniques for the relevant dynamical systems; the case of the molecule H_2^+ subjected to short laser pulses is used as an illustrative example. The two types of state are found to play different roles. The bound-state eigenvectors, relevant to the permanent regime, induce the dissociative flux transport when the laser field envelope varies slowly and ensure globally the correct integrated quantum flux. The discretized pseudo-scattering states associated with the transitional regime are relevant for sudden variations of the laser field envelope and govern the time dependence of the asymptotic dissociative flux by temporarily increasing or decreasing the flux transported by the states in the first group of Floquet resonance states. A detailed study shows that the lifetimes of the pseudo-scattering eigenvectors (which are generally regarded as somewhat arbitrary in the complex absorbing potential model) do have important physical relevance.

PACS numbers: 03.65.Nk, 02.30.Tb, 02.60.-x, 03.65.-w, 31.15.p

1. Introduction

Adiabatic techniques are used to describe photoreactive processes within the context of Floquet theory when some of the laser field parameters do not vary too rapidly. These techniques generally introduce approximations to deal with nonadiabatic couplings and often limit the size of the active Hilbert spaces selected to implement a discretized approach. Guérin and Jauslin [1], for example, proposed an adiabatic Floquet method by assuming only localized nonadiabatic effects, in the sense that the adiabatic transport can be considered as made up of lengthy adiabatic passages along eigenstate trajectories plus local diabatic evolutions near conical intersections. In another approach, by Dresse and Holthaus [2], the nonadiabatic couplings are incorporated by using first-order perturbation theory. The high-frequency limit approach developed by Gravila [3] is yet another technique which attempts an adiabatic approach.

The concept of an active subspace containing the major part of the wavefunction evolution appears in the approach of Guérin and Jauslin [1], which is based on the quantum analogue of the Kolmogorov–Arnold–Moser (KAM) transformation. The related concept of an effective Hamiltonian is implicit in the superadiabatic Floquet approach [2, 4] which produces bases which follow any nonadiabatic evolution. It is, of course, explicit in the time-dependent wave operator theory (TDWOT) which is also used in the numerical treatment of photoreactive processes [5] to expand the wavefunction of an open system on instantaneous Floquet eigenvectors (cf equation (7.10)–(7.12) of [5]). Fleischer and Moiseyev [6] propose a similar expansion (their equations (34)–(36)) but employing a principally different approach which consists of the derivation of an adiabatic theorem for open systems and giving an analytical criterion for the validity of the adiabatic limit with the help of the (t, t') formalism combined with the complex scaling method.

A purely adiabatic treatment using a one-dimensional space enables an evident reducing of the computational time required to perform the integration of the dynamical equations for photoreactive processes involving large molecules. By making these processes dependent on the properties of a single Floquet resonance state, this treatment makes it easier to understand how to control the processes in function of the laser field parameters. A crucial point is the size and content of the selected active space, particularly when localized rapid time evolutions of the laser field parameters occur between lengthy adiabatic passages. The fundamental question of this intermediate situation is whether the adiabatic approach has to be completely abandoned or it can be conserved to some extent.

This question has been partly answered by Fleischer and Moiseyev [6] from the viewpoint of an analytical criterion for the shape and duration of the laser pulse for which the system is controlled by a single resonance Floquet state. The present paper addresses the choice of the active space of relatively small dimension which replaces the single state of traditional adiabatic theory. It is focused on the complete integration of the Schrödinger equation by using both a discretized scheme with respect to the time-dependent adiabatic parameters and the direct calculation of the instantaneous Floquet eigenvectors. Another fundamental difference with the study of [6] concerns the nature of the non-adiabaticity. Fleischer and Moiseyev consider Floquet eigenstates issued from the bound states or from shape and Feshbach resonances of the field-free molecule. These states dressed by the electric field are independent of the complex rotation when the scaling parameter is sufficiently large and contribute to the dynamics when they overlap with the initial bound state also dressed by the field. Such a situation appears even for slow variations of the adiabatic field parameters and is related to the accidental near resonances created by the field dressing. This type of non-adiabaticity is not however present for the H_2^+ ion case where direct transitions from the ground surface to an upper structureless

surface occur and the simple space of a single resonance is sufficient to describe the dynamics. In contrast, a principally different kind of adiabaticity defects appears in this system when the time evolution of the parameters includes some fast changes which generate direct projections of the wavefunction into the scattering states of the upper continuum. These effects have to be accounted for when the use of finite bases and the discretization of the continua require the introduction of complex transformations in order to reproduce the non-Hermitian character of the Hamiltonian. The use of an optical potential strongly modifies the ‘pseudo-scattering’ states which discretize the continua and produces large imaginary parts in the eigenvalues of these modified scattering states. An important question arises then about the role of these modified states. Do these states directly contribute to the transport of the quantum flux or they have an indirect and more subtle role in the simulation of the continuum projection of the wavefunction? In order to answer exhaustively this question, we investigate both the composition and the smallest possible dimension of the active space necessary to reproduce the time-dependence of the flux and of the wavefunction throughout the duration of the reactive process.

The paper is organized as follows. Section 2 describes some aspects of the adiabatic transport formula and of the Floquet theory and combines the adiabatic transport theory, the Floquet theory and the time-dependent wave operator concept to obtain a discrete expression for the time evolution of the wave packet inside a reduced active space of the extended Hilbert space. Section 3 uses this result to describe photoreactive processes for different laser pulses and compares the resulting approximate expressions with ‘exact’ wave packet calculations in the case of H_2^+ . For such a simple system the dynamical equations can, of course, be integrated more directly, so that the adiabatic formalism, although not facing a severe test, can have its numerical results compared with the exact ones. In addition, the small size of the system makes easier to understand the role played by each basis vector, with the possibility of extrapolating to larger systems. A particular attention is paid consequently to investigating how the different eigenstates of the active space contribute to the construction of the wavefunction in the adiabatic and in the sudden regimes. Section 4 provides a summary of the main results and some conclusions.

2. An adiabatic transport formula and time-dependent wave operator theory for cyclic evolutions

2.1. A summary of the problem

The semi-classical picture of the interaction of a laser pulse with a molecule makes use of a periodic or a quasiperiodic Hamiltonian. For a dissociation process the Hamiltonian of the system is taken to be

$$H(t) = H_0 + \mu f(t) \sin[\omega(t)t], \quad (1)$$

where H_0 is the Hamiltonian of the free molecule, μ is the electric dipole, $f(t)$ is the field envelope and $\omega(t)$ is the instantaneous radiation frequency.

With such a quasiperiodic Hamiltonian the number of H_0 -eigenvectors required to describe the dynamical process is very high and the standard adiabatic theorem cannot be applied directly. To describe the dynamics it is first necessary to separate the fast oscillating terms from the slow adiabatic evolution of the parameters $f(t)$ and $\omega(t)$. To this end we introduce the phase ϕ , which obeys the equation

$$\frac{\partial \phi(t)}{\partial t} = \omega_{\text{eff}}(t) = \omega(t) + \dot{t} \quad (2)$$

and then write the Hamiltonian $H(t)$ as

$$H(s, \phi) = \frac{T}{\hbar\omega_{\text{eff}}(s)} [H_0 + \mu f(s) \sin(\phi)], \quad (3)$$

where $s = t/T$ is the reduced time defined by the pulse duration T . By doing this, we introduce a theory involving two-time variables as did Breuer and Holthaus [7] and Peskin and Moiseyev [8].

To complete the description of the adiabatic dynamics by means of the parameters $f(s)$ and $\omega_{\text{eff}}(s)$ it is necessary to develop the adiabatic transport formula within this two-time variable framework, and also to select in a self-consistent manner the model space used to construct the successive active spaces in which the dynamics is concentrated. This model subspace, characterized by the projector P_0 , is imbedded in a large extended Hilbert space $\mathcal{H} \otimes L^2(S^1, d\theta/2\pi)$ which is a product of the bare molecule Hilbert space and the space of square integrable functions on the circle of length 2π [1, 2, 9]. The selection of this subspace can be made efficiently by using the wave operator sorting algorithm proposed by Wyatt and Jung [10], which considers the wave operator associated with the initial state.

The generalization of this formalism to the extended Hilbert space with a two-time variable Hamiltonian is the subject matter of a theorem demonstrated in [11] which can be summarized as follows.

Let $X(\phi)$, the reduced wave operator in \mathcal{H} , be a solution of the equation [5]

$$i\partial_\phi X(\phi) = (1 - X(\phi))H(\phi, \phi)(1 + X(\phi)). \quad (4)$$

This reduced wave operator $X(\phi)$ is the operator which defines the effective Hamiltonian $H^{\text{eff}} = P_0 H (P_0 + X)$ which drives the dynamics projected into the active subspace. Let $X_F(\phi, s)$, the reduced wave operator in $\mathcal{H} \otimes L^2(S^1)$, be a solution of the equation

$$i\partial_s X_F(\phi, s) = (1 - X_F(\phi, s))H_F(s, \phi)(1 + X_F(\phi, s)), \quad (5)$$

with the Floquet Hamiltonian

$$H_F(s, \phi) = H(s, \phi) - i\partial_\phi.$$

Then $X_F(\phi, \phi)$ is a solution of equation (4), so that $X_F(\phi, \phi) = X(\phi)$.

In the context of the two-time variable theory, this theorem indicates that it is possible to put the emphasis on the adiabatic behaviour by considering the Floquet Hamiltonian H_F defined in the extended Hilbert space. The final result is a dynamical equation (equation (5)) which refers to the domain of the slow-time variable s and which involves a derivative with respect to this time variable only. The theorem then justifies the use, at the adiabatic limit, of a Floquet treatment as well as its combination with both an adiabatic transport formula to manage the dynamics and a time-dependent wave operator formulation to select the subspace in which the dynamical evolution takes place. The instantaneous Floquet eigenstates, i.e. the eigenvectors of $H_F(s, \phi)$ for a fixed value of s , then appear as a natural basis set.

2.2. The Aharonov non-adiabatic transport equation and its discretized version

By freezing the s -dependence, the Floquet Hamiltonian $H_F(s, \phi)$ becomes purely periodic. Aharonov and Anandan [12] found that the usual adiabatic transport formula can be generalized to such a non-adiabatic periodic case. Viennot *et al* [13, 14] derived recently a non-Abelian and non-adiabatic transport formula by introducing the Floquet eigenstates $|\lambda_b(t)\rangle$ such that

$$\Psi(t) = \sum_b [\mathbf{T} e^{-i\hbar^{-1} \int_0^t E_\lambda(t') dt' - \int_0^t A(t') dt'}]_{ba} |\lambda_b(t)\rangle, \quad (6)$$

with

$$H_F(t, \phi)|\lambda_b(t, \phi)\rangle = \lambda_b(t)|\lambda_b(t, \phi)\rangle.$$

This equation had been already given in the topical review [5] (equation (7.11) of [5]), and is equivalent to equations (34)–(37) of [6] even if the theoretical developments and the writings are quite different. The term $[\cdots]_{ba}$ is the matrix element of the time-ordered exponential of the time integral of two matrices $(i\hbar)^{-1}E$ and A . The first term is the dynamical phase corresponding to the diagonal Floquet eigenvalue matrix $E_{ij}(t) = \lambda_i(t)\delta_{ij}$, the second one is a non-Abelian and non-adiabatic Berry phase with $A_{ij}(t) = \langle \lambda_i(t) | \partial \lambda_j(t) / \partial t \rangle$. The geometric description of the non-Abelian Berry phase has also been introduced in [15].

We assume that, at each instant, the evolution obeys an adiabatic theorem inside an active space constructed on the reduced basis set $\{|\lambda_a(t)\rangle\}_{a=1,\dots,m}$, i.e.

$$\forall t, t': U(t, t')P_m(t') = P_m(t)U(t, t'), \quad (7)$$

where U is the quantum time evolution associated with H_F and $P_m(t)$ is the projector constructed using the reduced basis $\{|\lambda_a\rangle\}$ and the associated biorthogonal basis set $\{|\lambda_a^\dagger\rangle\}$:

$$P_m(t) = \sum_{a=1}^m |\lambda_a(t)\rangle \langle \lambda_a^\dagger(t)|. \quad (8)$$

If we consider a discrete partitioning of the time interval, $\{t_0 = 0 < t_1 < \cdots < t_N = t\}$, we can derive a discrete version of the continuous transport formula (equation (6)) in the form [14]

$$\Psi(t) = \sum_{b=1}^m \left[\mathbf{T} \prod_{i=1}^{N-1} \mathbf{R}(i+1, i) e^{-i\hbar^{-1}E(t_i)\Delta t_i} \right]_{ba} |\lambda_b(t)\rangle, \quad (9)$$

where $\Delta t_i = t_{i+1} - t_i$ and where $\mathbf{R}(i+1, i)$ is the overlapping matrix between the basis set at time t_i and the associated biorthogonal basis set at time t_{i+1} ,

$$\mathbf{R}(i+1, i) = \begin{pmatrix} \langle \lambda_1^\dagger(t_{i+1}) | \lambda_1(t_i) \rangle & \cdots & \langle \lambda_1^\dagger(t_{i+1}) | \lambda_m(t_i) \rangle \\ \vdots & \ddots & \vdots \\ \langle \lambda_m^\dagger(t_{i+1}) | \lambda_1(t_i) \rangle & \cdots & \langle \lambda_m^\dagger(t_{i+1}) | \lambda_m(t_i) \rangle \end{pmatrix}. \quad (10)$$

In equations (8)–(10), the biorthogonal basis set is introduced in order to take into account the dissipative character of the photoreactive process.

Equations (9)–(10) are derived in a rigorous fashion in [14]. The derivation reveals that the transition from the continuous transport formula to the discrete ones generates errors proportional to both the second derivatives $\frac{\partial^2}{\partial t^2} |\lambda_j(t, \phi)\rangle$ and to $(\Delta t_i)^2$. It also reveals that the passage from the continuous to the discrete limit is rigorous (and consequently does not induce any error) if a second hypothesis is added to the adiabatic assumption (equation (7)), i.e. if one assumes that the time functions which define the adiabatic parameters $f(t)$ and $\omega(t)$ are step functions (this approximation is usual in the continuous integration of the Schrödinger equation). In this case the discrete instants t_i correspond to the transition instants from one stage to the next: $f(t_i - \epsilon) = f \rightarrow f(t_i + \epsilon) = f + \Delta f$ and $\omega(t_i - \epsilon) = \omega \rightarrow \omega(t_i + \epsilon) = \omega + \Delta \omega$.

It is straightforward to establish the rigorous character of the propagation scheme when step functions are used for the adiabatic parameters. The adiabatic assumption (equation (7)) implies the existence of an initial active space $S^{(t=0)}$ (the model space) exclusively determined by the initial molecular state and by the laser–matter interaction. This space is spanned by a group of m free Floquet eigenstates. For each new value taken by the set of the adiabatic parameters a new target space $S^{(t=k)}$ of the same dimension is formed by solving the degenerate

stationary Bloch equation $H_F \Omega = \Omega H_F \Omega$. The adiabatic approximation assumes that at each discontinuity of the parameters the wavefunction located in the subspace $S^{(t_k)}$ is completely projected into the following target subspace $S^{(t_{k+1})}$. By using the sudden approximation at the discontinuity t_k , namely

$$\lim_{\epsilon \rightarrow 0} \Psi(t_k - \epsilon) = \lim_{\epsilon \rightarrow 0} \Psi(t_k + \epsilon) \quad (11)$$

and by taking advantage of the adiabatic assumption, we obtain, without any supplementary approximation, a formula which is consistent with equation (9), namely the result

$$\begin{aligned} \lim_{\epsilon \rightarrow 0} |\Psi(t_k + \epsilon)\rangle &= \lim_{\epsilon \rightarrow 0} \sum_{l=1}^m \sum_{j=1}^m |\lambda_l(t_{k+1})\rangle \langle \lambda_l^\dagger(t_{k+1}) | \lambda_j(t_k) \rangle \langle \lambda_j^\dagger(t_k) | \Psi(t_k - \epsilon)\rangle \\ &= \lim_{\epsilon \rightarrow 0} \sum_{l=1}^m \left[\sum_{j=1}^m \mathbf{R}_{l,j}(k+1, k) \langle \lambda_j^\dagger(t_k) | \Psi(t_k - \epsilon)\rangle \right] |\lambda_l(t_{k+1})\rangle. \end{aligned} \quad (12)$$

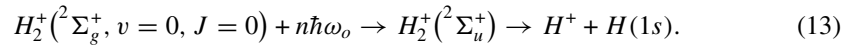
On the other hand, the propagation along the plateau $f(t) \equiv f$ and $\omega(t) \equiv \omega$ between t_k and t_{k+1} induces pure phase terms, since the working basis is composed of rigorous eigenstates of H_F . These phases are the dynamical phases which appear in equation (9).

3. Analysis of the H_2^+ photodissociation

The particular case of H_2^+ photodissociation is worthy to be investigated for two goals. The first goal is to illustrate a non-adiabaticity relevant to localized fast variations of the adiabatic parameters which produce a direct projection of the wavefunction into the pseudo-scattering states describing the continuum (i.e. the second type of non-adiabaticity described in the introduction). In this case the Floquet eigenstates participating in the photodissociation are the initial dressed bound state (whose eigenvalue is independent of the optical potential) and some pseudo-scattering states in near resonance with this bound state (whose eigenvalues depend on the optical potential). The subtle role of these pseudo-scattering states can be therefore elucidated for the case where fast variations of the field amplitude destroy the adiabaticity. The second goal is to propose a new integration scheme of the Schrödinger equation. In [6] (equation (53)) the adiabaticity criterion which defines the dimension and the composition of the active subspace assumes the knowledge of all the adiabatic Floquet eigenstates of the states describing the interaction with a cw laser (named here ‘instantaneous Floquet eigenstates’) and employs the diagonalization of the Floquet Hamiltonian. This procedure is unfortunately untractable in numerous cases because of too large representation basis required for computation. We present here, in contrast, a complete integration of the Schrödinger equation by using both a discretized scheme with respect to the time-dependent adiabatic parameters (equation (9)) and a direct calculation of the Floquet eigenvectors composing the successive active subspaces.

3.1. Description of the system

The photodissociation of H_2^+ involves an excitation step and a dissociation step:



The total molecule-plus-field Hamiltonian, within the Born–Oppenheimer and dipole approximations, is written in the so-called length gauge. The electronic potential energies $V_g(R)$, $V_u(R)$ of the $\ ^2\Sigma_g^+$ and $\ ^2\Sigma_u^+$ states, respectively, as well as the transition dipole $\mu(R)$,

are taken from the paper of Bunkin and Tugov [16]. The laser is characterized by its carrier wave frequency $\omega_o = 0.295\,868$ au (corresponding to a wavelength $\lambda_o = 154$ nm) and its pulse shape $E(t)$ defined by the Gaussian envelope function

$$E(t) = \begin{cases} \epsilon_o \exp\left[-\left(\frac{t-t_1}{\tau}\right)^2\right] & \text{for } t \leq t_1 \\ \epsilon_o & \text{for } t_1 \leq t \leq t_2 \\ \epsilon_o \exp\left[-\left(\frac{t-t_2}{\tau}\right)^2\right] & \text{for } t \geq t_2, \end{cases} \quad (14)$$

with a maximum amplitude ϵ_o corresponding to the intensity $I = 10^{12}$ W cm⁻². The time parameters t_1 , t_2 and τ are chosen to produce an adiabatic or a sudden regime, as explored in this study. Two cases have been studied in detail and are presented here. The first, called an adiabatic case, corresponds to a pure Gaussian pulse ($t_2 - t_1 = 0$), with a rise time $\tau = 5000$ au and a pulse duration $T = 30\,000$ au. The second introduces more sudden variations of the laser pulse and is characterized by $t_2 - t_1 = 1033.527$ au, a rise time $\tau = 50$ au and a total pulse duration equal to 3000 au.

3.2. The active subspaces in the discretized Floquet scheme

The discrete transport formula is given by equation (9). Our application introduces into this equation a single adiabatic parameter—the amplitude $E(t)$ of the laser field. We note that the descriptive adjective ‘adiabatic’ is retained. It is appropriate to the contents of section 2.1 and of equation (3), even if $E(t)$ shows sudden but localized variations.

The discrete character of the dynamics results from a partitioning of the amplitude; the range $[0, \epsilon_o]$ is divided into 100 steps of equal amplitude, producing 101 discrete values,

$$E_j = \frac{j \times \epsilon_o}{100}, \quad j = 0, \dots, 100. \quad (15)$$

The transition instants t_j are chosen as the instants corresponding to the values $E(t) = (E_{j+1} + E_j)/2$ when the field increases from E_j to E_{j+1} or decreases from E_{j+1} to E_j . A zeroth-order basis is constructed for each of the two surfaces by taking the tensorial product $\{|v\rangle \otimes |n\rangle\}$ of radial functions $|v(r)\rangle$ and of Fourier time functions $|n\rangle$ with $\langle t|n\rangle = \exp(in2\pi t/T)$. A radial basis of N_r ($N_r = 150$) Fourier functions $|v_k(r)\rangle = \exp(i2\pi kr/L)$ is used to span the radial range ($r = 0$, $r = L = 18$ au) and to propagate the wave packet in the time integration of the Schrödinger equation. An equivalent basis is formed by the 150 first eigenvectors of $H_0 - iV_{\text{opt}}(r)$ in the adiabatic Floquet treatment. $N_F = 4$ Fourier time functions $|n\rangle$ are used. They correspond to the initial state of the field ($n = 0$, by convention), the states describing the absorption of one photon ($n = -1$) and two photons ($n = -2$) as well as the state associated with the creation of one photon ($n = 1$) during the field–matter interaction. This small number of Floquet blocks is sufficient in the present case because of the laser frequency and amplitude used.

The initial model space $S^{(t=0)}$, which corresponds to a laser field amplitude equal to zero, is spanned by m non-perturbed states $\{v, n\}$. The initial state ($v = v_i$, $n = 0$) is the first element of this group of m states. (The choice $n = 0$ assumes an initial averaged phase between the molecule and the laser field.) The selection of this space has a central importance, since the time dynamics evolves in successive active spaces which issue from $S^{(t=0)}$ as the laser field increases. By using the wave operator sorting algorithm [10], one can reorder all the non-perturbed states $\{v, n\}$ (the initial state being in first position) and construct an m -dimensional model space by selecting the m first reordered states.

We believe that the states selected with the highest priority by this sorting algorithm are the same that the states which would be selected by the adiabaticity criterion of Fleischer and

Table 1. The 25 first states ($1 \leq N \leq 25$) selected to construct the model space. The symbol $s = 1, 2$ denotes, respectively, the energy surfaces, ${}^2\Sigma_g^+$ and ${}^2\Sigma_u^+$. n ($-2 \leq n \leq 1$) is the number of the Floquet block and v ($0 \leq v \leq 149$) is the number of the vibrational state (these vibrational states are bound states in the case $s = 1$ and $n \leq 18$ or $(H_0 - iV_{\text{opt}})$ -eigenstates of the discretized continuum).

N state number	s surface	n Floquet block	v vibration	Eigenvalues
1	1	0	0	$-0.972891(-01) - i 0.282762(-15)$
2	2	-1	90	$-0.956967(-01) - i 0.266023(-02)$
3	2	-1	89	$-0.996642(-01) - i 0.271068(-02)$
4	2	-1	91	$-0.916935(-01) - i 0.260854(-02)$
5	2	-1	88	$-0.103596(+00) - i 0.275989(-02)$
6	2	-1	92	$-0.876548(-01) - i 0.255564(-02)$
7	2	-1	93	$-0.835805(-01) - i 0.250154(-02)$
8	2	-1	94	$-0.794706(-01) - i 0.244624(-02)$
9	2	-1	87	$-0.107493(+00) - i 0.280784(-02)$
10	2	-1	95	$-0.753251(-01) - i 0.238977(-02)$
11	2	-1	96	$-0.711440(-01) - i 0.233212(-02)$
12	2	-1	97	$-0.669272(-01) - i 0.227331(-02)$
13	2	-1	98	$-0.626747(-01) - i 0.221335(-02)$
14	2	-1	99	$-0.583866(-01) - i 0.215225(-02)$
15	2	-1	86	$-0.111353(+00) - i 0.285451(-02)$
16	2	-1	100	$-0.540627(-01) - i 0.209002(-02)$
17	1	0	1	$-0.870537(-01) - i 0.860805(-16)$
18	2	-1	101	$-0.497030(-01) - i 0.202666(-02)$
19	2	-1	102	$-0.453074(-01) - i 0.196220(-02)$
20	2	-1	103	$-0.408760(-01) - i 0.189663(-02)$
21	2	-1	104	$-0.364085(-01) - i 0.182999(-02)$
22	2	-1	105	$-0.319051(-01) - i 0.176228(-02)$
23	2	-1	106	$-0.273655(-01) - i 0.169352(-02)$
24	2	-1	107	$-0.227897(-01) - i 0.162373(-02)$
25	2	-1	108	$-0.181776(-01) - i 0.155294(-02)$

Moiseyev [6]. Our sorting algorithm is based on the recursive distorted wave approximation method whose iterative factors are similar to those of the adiabaticity criterion (equation (43) of [6]). The 25 first selected states corresponding to $v_i = 0$ are listed in table 1. The table reveals that the model space is constituted essentially of ‘pseudo-scattering’ states which discretize the upper surface. These states dressed by the laser field are in near resonance with the initial dressed state ($v = 0, n = 0$); the energy difference between each state of the model space and the initial dressed state increases with the ordering number N . Apart from the ground bound state, only the first excited bound state ($v = 1, n = 0$) is present (in the 17th place). This is confirmed by figure 1 which represents the energy eigenvalues of the field-free Floquet Hamiltonian which are closest to the initial state. The figure shows a part of the branch ($n = 0$) with the two selected bound states ($v = 0, n = 0$ and $v = 1, n = 0$) and a part of the branch ($n = 1$) with the 23 other states which constitute the largest model space selected in this study. A more detailed analysis of the full spectrum on larger scales reveals that the two ‘pseudo-continua’ corresponding to ${}^2\Sigma_g^+$ and ${}^2\Sigma_u^+$ are nearly identical in the complex plane, both having a periodicity equal to $\hbar^{-1}\omega_o = 0.295868$.

This figure also reveals that the value of the energy shift with respect to the initial state is not the dominant determining factor in the selection of the model space in this weak coupling

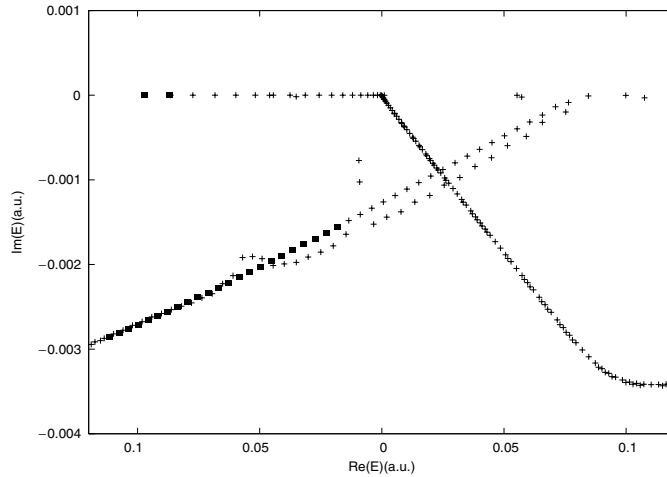


Figure 1. Ensemble of energy eigenvalues of the field-free Floquet Hamiltonian of H_2^+ , closest to the initial state ($v = 0, n = 0$). The 25 first states selected to construct the model space are represented by black squares, the other states by crosses.

regime. If the bound states ($v \geq 2, n = 0$) which are close to the initial state ($v = 0, n = 0$) are not selected, this is simply because the transitions ($v = 0, n = 0$) \rightarrow ($v \geq 2, n = 0$) require a second-order perturbative expansion. In fact the composition of the model space strongly depends on the field amplitude. Tests have revealed that if one multiplies the laser amplitude ϵ_o by five then several bound states are selected in priority before the ‘pseudo-continuum’ states.

It is important to note that the dressed unperturbed bound states have real eigenvalues (the small imaginary parts $< 10^{-15}$ come from the finite numerical precision). In contrast, the scattering states modified by the absorbing potentials (placed asymptotically on each surface) possess complex eigenvalues with large imaginary parts $> 10^{-3}$.

3.3. The discretized dynamical scheme

When the model space has been selected, the recursive distorted wave approximation (RDWA) method is used to calculate the m -dimensional bases of the 100 successive active spaces $\{\lambda_{(v,n)}^{E_j}\}$ corresponding to the 100 discretized values E_j of the laser field (see equation (15)).

In our notation, a convenient labelling of the Floquet eigenstates $|\lambda_{v,n}^{E_j}\rangle$ is produced by using the two indices referring to the non-perturbed system. This choice assumes a state-to-state correspondence between the non-perturbed states (eigenvectors of $H_0 - iV_{\text{opt}} - i\hbar\partial/\partial t$) and the Floquet eigenstates, namely $(v, n) \longleftrightarrow \lambda_{v,n}$. For the intensity range investigated in this paper, this assumption does not pose any difficulty. By starting from the selected model space and by considering the 100 electric-field amplitudes one after the other, from $\epsilon_o/100$ up to ϵ_o , we derive each new active space basis set by taking as input for the RDWA iteration calculation the basis set for the preceding amplitude. At the end of each RDWA-iteration the two ingredients which appear in equation (9), the overlapping matrix \mathbf{R} and the Floquet eigenvalues E_λ , are stored in memory.

The shape of the laser-field envelope appears in equation (9) only via the widths of the plateaus Δt_i of the step function which represents the field amplitude. When the overlapping

matrices and the groups of Floquet eigenvalues are stored, the final calculation is very fast, particularly if the dimension m of the model space is very small compared with the full dimension of the extended Hilbert space. Our treatment is thus well adapted to repeat a large number of calculations for different pulse shapes possessing a maximum amplitude $E_{\max} \leq \epsilon_0$, since all these calculations share the same overlapping matrices \mathbf{R} and the same Floquet eigenvalues. The total CPU time per simulated experiment is about the same as that used for the direct integration of the Schrödinger equation in the case of the short pulse $T = 3000$ au, but it is five time smaller for the long pulse, $T = 30\,000$ au. One can then expect a very large reduction factor (>100) of the CPU time required for nanosecond pulses.

This comparison nevertheless requires some comments about the absorbing potential method, the direct integration method, called ‘exact’ in our approach and the status of the present adiabatic solution.

First, in both the discretized dynamical scheme and the direct integration of the Schrödinger equation, a complex absorbing potential $-i\eta V_{\text{opt}}(r)$ has been introduced on the two surfaces ${}^2\Sigma_g^+$ and ${}^2\Sigma_u^+$ in order to absorb the outgoing flux produced by the dissociation. Compared with the complex scaling method, the major advantage of this method is its simplicity. Following Riss and Meyer [17] the eigenspectrum of the perturbed Hamiltonian $H - i\eta V_{\text{opt}}$ coincides with the resonance poles, provided that a complete basis set has been used. Since in our calculations a finite (and thus incomplete) basis spans the finite interval $[0, L]$, artificial reflections are introduced. Different methods, using perturbation theory [18] or Padé extrapolation technique [19], have been used to remove the artificial reflection effect for finite values of η . Further, two different approaches have been developed to address the question of the existence of a complex absorbing potential (CAP) which possesses a finite non-perturbative strength and yet does not produce any reflection. A reflection-free CAP has been combined by Moiseyev with the smooth-exterior scaling transformation [20], and Riss and Meyer looked for the similarity transformation which provides a reflection free CAP, identical under certain specific approximation to a non-local, kinetic-type operator [17]. In the present study such sophisticated procedures have not been used inasmuch as high-order convergences are unnecessary. We have thus introduced two identical absorbing complex potentials $-i\eta r^{-16}$ with finite asymptotic amplitudes on the two surfaces, as did Jolicard and Austin [21]. By varying the amplitude η we have converged the two perturbed resonance eigenvalue results up to two digits for each of the 100 discrete values of the laser field (these resonances correspond to the two bound states ($N = 1$) and ($N = 17$) in table 1) and verified *a posteriori* that the asymptotic integrated quantum flux values in figures 5 and 11 were insensitive to small variations of the absorbing potential amplitude.

Second, the term ‘exact’, used to designate a direct integration of the time-dependent Schrödinger equation with a wave packet propagation scheme is, strictly speaking, not correct, since both the finite basis set and the propagation scheme introduce approximations. For the present fast varying time-dependent Hamiltonian, a global propagator associated with long-time steps is inappropriate. We have thus used a second-order differencing (SOD) scheme, with a symmetric modification of the expansion in order to conserve the time reversal symmetry of the Schrödinger equation

$$\Psi(t + \Delta t) \approx \Psi(t - \Delta t) - \frac{2i}{\hbar} \Delta t H \Psi(t).$$

As this scheme is only stable if the Hamiltonian operator is strictly Hermitian, the absorbing potentials $-i\eta V_{\text{opt}}(r)$ have been extracted from H and used separately, after each propagation scheme, as in a split operator method,

$$U(\Delta t) = \exp(-\eta V_{\text{opt}} \Delta t / \hbar) U_{\text{SOD}}(\Delta t).$$

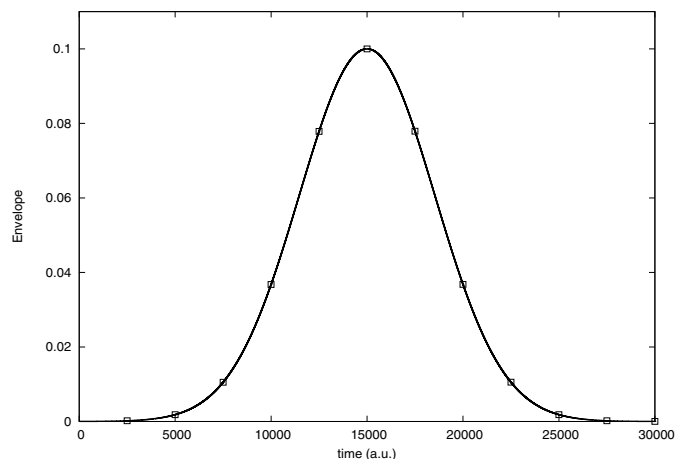


Figure 2. Adiabatic laser pulse shape.

The stability of the SOD scheme was first tested without complex absorbing potentials. The theory indicates a stability criterion which requires $\Delta t < \hbar/E_{\max}$, where E_{\max} is the eigenvalue with largest absolute value of the discrete Hamiltonian operator. This stability was confirmed by our tests. Then the stability of the splitting method was tested with success by varying the amplitude of the complex absorbing potential.

Finally, concerning the status of our solution, it should be recalled that equation (9) is an approximate solution, within an adiabatic dynamical scheme, and so cannot give an exact solution. Its use is possible only if the dynamics is describable using a series of connected small active spaces. The following sections reveal that this assumption, perfectly satisfied for an adiabatic pulse, leads to active spaces of increasing sizes (and thus to increasing CPU times) when pulses with fast variations are used. Another difficulty for the method is the calculation of the perturbed Floquet eigenvectors when the electric field takes large values, owing to the existence of dense complex spectra.

Nevertheless the advantage of our approach is undeniable in some precise circumstances: when very long adiabatic pulses of weak amplitudes interacting with complicated molecular systems are used and when the repetition of experiments corresponding to various pulse shapes of the same maximum amplitude is demanded by the photoreactive control experiment. This advantage lies in the discretization procedures which in both cases involves completely different variables. In equation (9), the integration steps correspond to a partition of the manifold of the adiabatic parameters (here the field amplitude). The basic operation at step (i) forms a product by the matrix $R(i + 1, i)$ (see equation (10)). In the usual integration of the Schrödinger equation, the steps correspond to a partition of the time and the basic operation at step (i) forms a product $H(t_i)\Psi(t_i)$. In adiabatic circumstances the basic CPU time of the first operation is very small compared with the CPU time of the second, because the size of the active space is small. Moreover the ratio of the two-step numbers tends rapidly to zero under the same circumstances; the benefit with respect to CPU time becomes very important.

3.4. Adiabatic pulse

The adiabatic pulse used is a pure Gaussian pulse characterized by a total pulse duration $T = 30\,000$ au and a rise time $\tau = 5000$ au. The envelope is represented in figure 2. On this

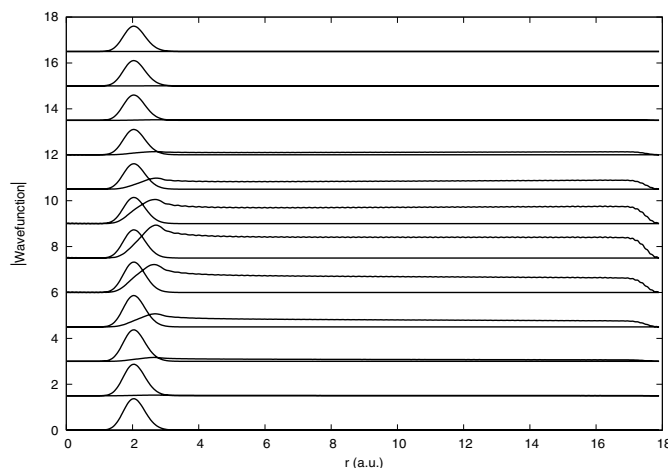


Figure 3. From top to bottom: moduli of the wavefunction corresponding to 12 ‘key’ instants of the adiabatic laser pulse. These results, obtained by a rigorous integration of the Schrödinger equation, show the partial components on the two electronic surfaces. Note that these components are not represented on the same scale (see the text).

figure the open squares denote the ‘key’ instants at which the wavefunction is calculated and plotted. To analyse the details of the photoreactive process in the framework of the discrete Floquet formulation, we present and compare the modulus of the wavefunction obtained by an exact integration of the Schrödinger equation with that obtained with equation (9) by working in the reduced m -dimensional active spaces. These comparisons are made at some ‘key’ instants represented in figure 2. A second analysis compares the time dependence of the integrated quantum flux at some asymptotic radial points, as obtained by the two calculations.

Figure 3 shows the wavefunction at the 12 ‘key’ instants of figure 2 uniformly distributed along the pulse envelope. The wave packet projected on the ground surface ${}^2\Sigma_g^+$ conserves the Gaussian shape which characterizes the ground state $v_i = 0$. When the laser amplitude takes non-negligible values an outgoing wave packet appears on the upper surface ${}^2\Sigma_u^+$ (note that these two partial wave packets are not represented on the same scale; a factor $50/3$ multiplies the components on the upper surface).

Figure 4 represents the same numerical experiment, but with results obtained from equation (9) by using a one-dimensional model space. Thus only the state number 1, i.e. the initial state ($v_i = 0, n = 0$) is selected in table 1 and the 100 subsequent active spaces are one-dimensional spaces. The comparison reveals that the envelope of the wavefunction is well reproduced by working in a succession of one-dimensional active spaces, namely those which are spanned at each time by the resonance state directly connected to the initial non-perturbed state. This situation is a pure adiabatic case, in the sense of ‘adiabatic’ used in [22]. This analysis is confirmed by the behaviour of the transition probabilities between the bound states of the ground surface. The transition probability $P_{0 \rightarrow 1}$ which increases during the interaction up to 10^{-4} , goes to zero when the field is turned off. Nevertheless the description ‘adiabatic’ here does not mean that nothing happens. A dissipative process is still involved, and it is the imaginary part of $E_{\lambda, v=0, n=0}$ in equation (9) which produces the decreasing of the norm from 1 to 0.647.

A small manifestation of non-adiabaticity subsists, nevertheless, when one studies the integrated quantum flux calculated at $r = 10.8$ along the excited surface (in the present

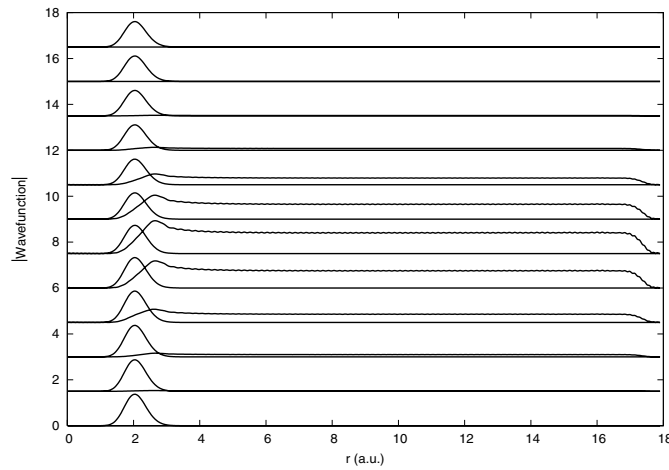


Figure 4. The same as figure 3, but the results are obtained by using equation (9) with a one-dimensional model space.

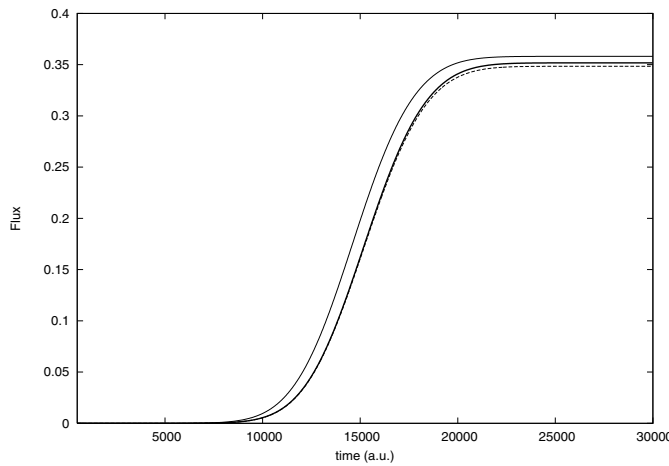


Figure 5. The asymptotic integrated quantum flux on the surface ${}^2\Sigma_u^+$ versus time. The deep continuous line corresponds to the rigorous integration of the Schrödinger equation. The thin continuous line results from the use of equation (9) with a one-dimensional model space. The dashed line corresponds to a model space of dimension 6.

experiment the outgoing flux along the ground surface ${}^2\Sigma_g^+$ is negligible). One can see in figure 5 a small displacement in time between the ‘exact’ quantum flux (i.e. the flux which results from the rigorous integration of the Schrödinger equation) and that obtained in our model by using a one-dimensional model space. This small discrepancy is removed if we work with a model space constructed by using the six first states of table 1.

3.5. Sudden pulse

The non-adiabatic effects are obviously more important with the second pulse, for which the rise time is drastically reduced. We will thus analyse the results of this second experiment

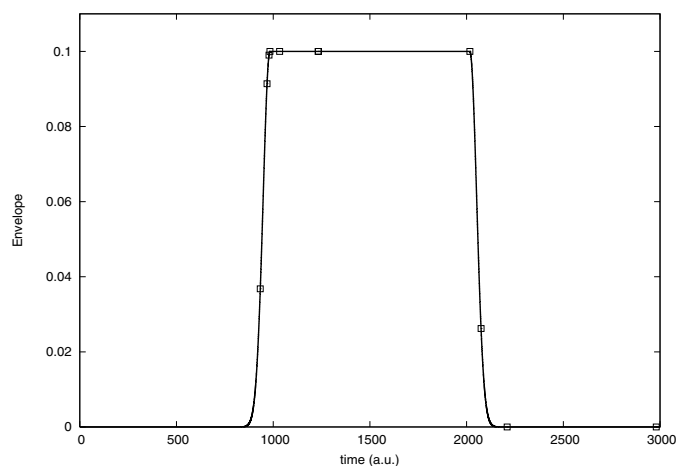


Figure 6. Sudden laser pulse shape.

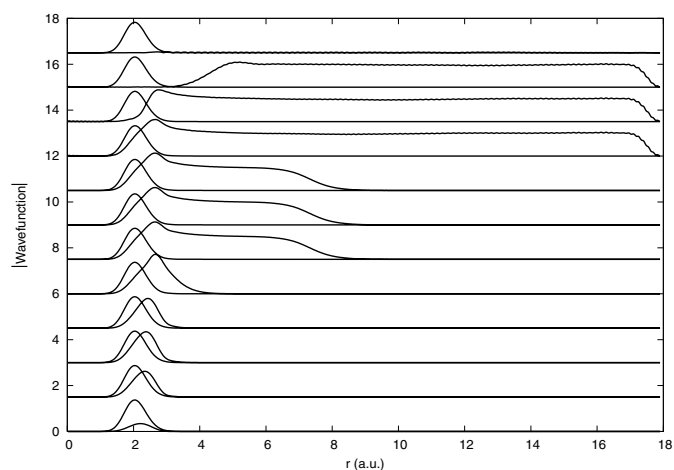


Figure 7. From top to bottom: moduli of the wavefunction corresponding to 12 'key' instants of the sudden laser pulse. These results, obtained by a rigorous integration of the Schrödinger equation, show the partial components on the two electronic surfaces. Note that these components are not represented on the same scale (see the text).

in detail before comparing the two experiments in an attempt to understand, in terms of the dimension and composition of the active spaces, the features which are associated with a sudden or an adiabatic regime.

The pulse shape is plotted in figure 6. In contrast with the preceding case, the 'key' instants are mainly placed at positions where the envelope shows a rapid increasing or decreasing behaviour. The wavefunctions obtained at the 12 'key' instants by a rigorous wave packet propagation are shown in figure 7. These results are quite different from those of figure 3.

In the adiabatic case (figure 3), the dissociative part of the wavefunction on the upper surface has, at each instant, an extension which covers the radial range ($0 < r < 18$ au) selected for our study. In the range ($16 \text{ au} < r < 18 \text{ au}$) one simply observes that the optical potential placed asymptotically absorbs this outgoing wavefunction. One can then easily

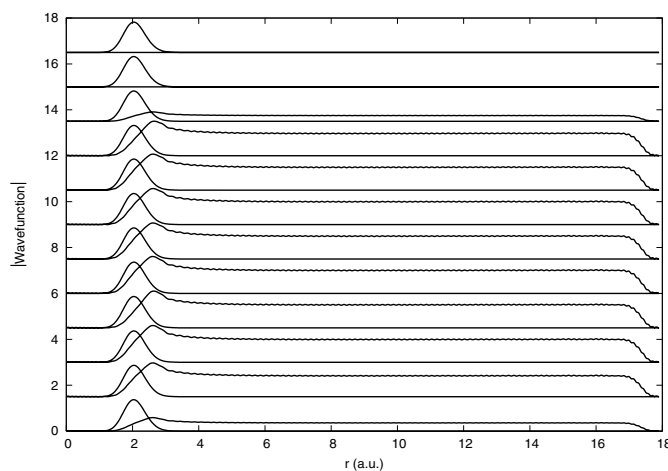


Figure 8. The same as figure 7, but with results obtained by using equation (9) with a one-dimensional model space.

understand that a unique Floquet state, in this case a resonance state created by the field–matter interaction from the initial dressed state ($v = 0, n = 0$), can correctly reproduce this behaviour. Indeed such a state has an infinite radial extension if a continuous description of the molecular continua is used. In the present discrete representation it extends over the finite selected range ($0 < r < 18$ au). In the sudden pulse case (figure 7) one observes transitional regimes near the instants at which the laser pulse envelope exhibits rapid variations. When the laser amplitude increases rapidly from zero up to the maximum value ϵ_o , the wave packet created above the initial bound state takes a finite time to propagate towards the dissociative plateau. Similarly, a large wave packet subsists after the laser field is turned off. Such a behaviour manifestly has a non-adiabatic character and cannot be reproduced by a unique resonance state with an amplitude increasing exponentially with the radial variable r outside the interaction region. This is confirmed by figure 8, which shows the result when we try to reproduce the wavefunction by using a series of one-dimensional active spaces. Because of the Siegert conditions satisfied by the resonance wavefunction one can see that, in contrast with figure 7, an asymptotic finite amplitude is created as soon as the laser field increases rapidly (in less than 100 au) from zero up to ϵ_o . The eight first wave packets (starting from the bottom) illustrate this difference perfectly. Similarly, the results at the ‘key’ points number 10 and 11, situated on the short region of rapid decrease of the laser amplitude, exhibit strong differences when comparing figures 7 and 8. The dissociative wave packet disappears on figure 8 as soon as the laser amplitude decreases to zero. In contrast, figure 7 shows a large amplitude of the dissociative wave packet. This residual amplitude should be understood as being due to the wave packet which is created during the large plateau ($1000 \text{ au} < t < 2000 \text{ au}$) and which continues to propagate towards larger r values. Only the ‘key’ instant number 9 situated at the end of the plateau gives similar wavefunction amplitudes in figures 7 and 8. This is, however, a special case, since the large plateau ($1000 \text{ au} < t < 2000 \text{ au}$) appears as an adiabatic interruption localized between fast evolutions.

A fundamental question is that of whether our discrete adiabatic transport formulation is able to describe these strongly non-adiabatic situations. Figures 9 and 10 show what happens when the size of the model space increases from 1 to 6 and from 6 to 21 by selecting the states given in table 1. With six states, important differences persist with respect to the exact

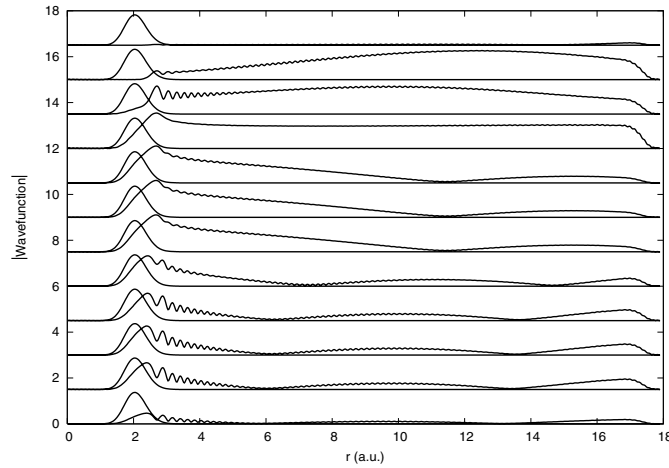


Figure 9. The same as figure 8 but with a model space constructed with the six first Floquet eigenvectors of table 1.

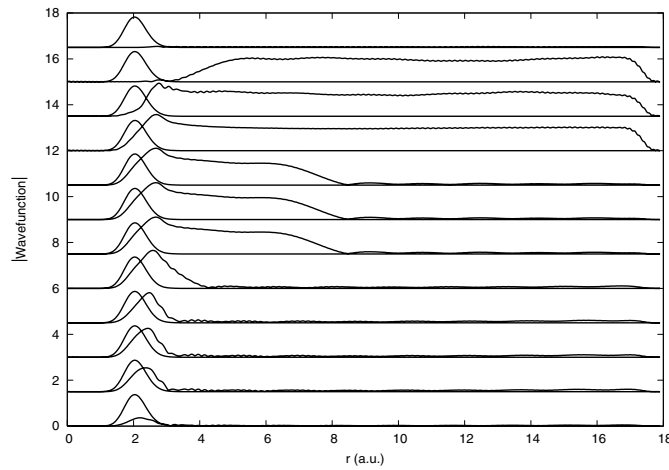


Figure 10. The same as figure 8 but with a model space constructed with the 21 first Floquet eigenvectors of table 1.

result, even if the general trend is correct: the five ‘pseudo-scattering’ states contribute to the disappearance of the asymptotic part of the wavefunction when the laser field increases rapidly from zero and, conversely, create an asymptotic wavefunction just after the turning off of the laser field. This trend is confirmed in figure 10. By using the 21 first states of table 1 we obtain results which are very similar to the exact ones. A comparison of figures 7 and 10 reveals small discrepancies, essentially weak spurious oscillations, in the inner part of the radial range. This result, of course, requires large active spaces. Nevertheless, it should be noted that this dimension is negligible when compared to the full dimension of the extended Hilbert space ($\mathcal{N} = 1200$) and that this constraint is produced by very fast variations of the laser envelope (see figure 6), which produce a significant broadening of the laser spectrum.

The capacity of the discrete non-Abelian transport equation (9) to describe this non-adiabatic situation is confirmed by analysing the integrated quantum flux (figure 11).

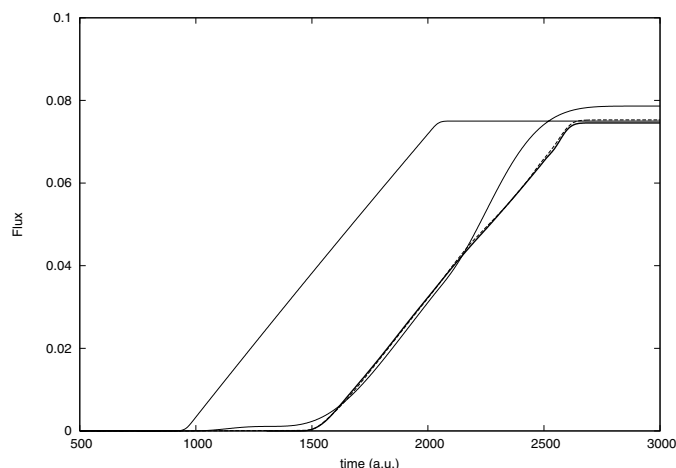


Figure 11. The asymptotic integrated quantum flux on the surface ${}^2\Sigma_u^+$ versus time. The deep continuous line corresponds to the rigorous integration of the Schrödinger equation. The two thin continuous lines result from the transport equation (9) with, respectively, one-dimensional and six-dimensional active spaces. The dashed line corresponds to the largest 21-dimensional active spaces.

By using a series of one-dimensional active space one observes a large displacement in time with respect to the exact results. The asymptotic flux appears 500 au earlier and disappears 500 au earlier. This defect is fully corrected by using a 21-dimensional active space and the time dependence of the integrated flux is well reproduced in detail: it is consequently difficult to distinguish between the deep continuous line and the dashed line in figure 11.

3.6. Role of the different eigenstates in describing adiabatic and non-adiabatic behaviour

The main goal of our calculations is to show that the discretized version of the transport equation can correctly reproduce the time evolution of the photoreactive process, even if the adiabaticity of this evolution is temporarily disturbed by some rapid variations of the laser parameters. In this case, the correct behaviour is obtained by taking into account, in addition to the resonance state $\lambda_{v=0, n=0}$ (which principally contributes to the total integrated flux), some ‘pseudo-scattering’ states selected in the model space. The following detailed analysis of the discretized equation (9) explains the role of these different contributions.

Equation (9) reveals that the evolution is a succession of transitions produced by the overlapping matrices \mathbf{R} and of dynamical phases produced by the \mathbf{E} matrices. It is the non-commutativity of these matrices which generates the complexity of the quantum evolution by augmenting at various times either the adiabatic or non-adiabatic character of the evolution.

When the field envelope varies very rapidly, by increasing from zero up to the plateau ϵ_0 or by decreasing from the plateau to zero (see figure 5), one can neglect the dynamical phases in the alternate products. equation (9) then gives rise to the products

$$\prod_{i=1}^{N-1} \mathbf{R}(i+1, i) \quad \text{or} \quad \prod_N^2 \mathbf{R}(i-1, i).$$

To be valid in this case, the adiabatic approximation (equation (7)) requires the use of large active spaces. Its introduction into the products gives

$$\prod_{i=1}^{N-1} \mathbf{R}(i+1, i) = \mathbf{R}(N, 1) \quad \text{and} \quad \prod_N^2 \mathbf{R}(i-1, i) = \mathbf{R}(1, N). \quad (16)$$

The resultant matrices $\mathbf{R}(N, 1)$ and $\mathbf{R}(1, N)$ induce large transition probabilities between the resonance state $\lambda_{v=0, n=0}^{i=N}$ ($\lambda_{v=0, n=0}^{i=1}$) and the $(m - 1)$ pseudo-scattering states of the active space which is associated with the smaller laser field amplitude ($i = 1$) (with the larger one ($i = N$)). Just after each fast variation of the field one can then observe a large dispersion of the wave packet over all the m states of the basis. We note that the introduction of equation (16) into equation (9) gives the same result as that obtained by using the sudden approximation. The criterion which justifies the use of this sudden approximation is (see equation (9))

$$\forall i \quad |\Delta E(t_i) \Delta t_i| \ll 1. \quad (17)$$

In the discretized scheme the values of the time interval Δt_i are limited both by the distance between the real energies and by the large imaginary parts of the energies of the continuous-discretizing states.

When the field envelope varies very slowly, as is the case with the adiabatic pulse (figure 2), a unique Floquet state is occupied during the experiment. The representation of this behaviour in the discretized scheme is simple. At each transition instant of the step function, the matrix \mathbf{R} induces small transition probabilities from the state number 1 (see table 1) up to the other states of the active space. However, the width of each step is very large at this adiabatic limit and the imaginary parts of the ‘pseudo-scattering’ states eigenvalues generate exponentially-decreasing terms which make these transitions disappear almost immediately. For the second non-adiabatic pulse (figure 6), a similar transitional effect appears at the beginning of the plateau and just after the end of the plateau. These transitional effects have a lifetime equal to the inverse of the imaginary part of the ‘pseudo-scattering’ state eigenvalues (in the present case it is equal to about 200 au). This lifetime characterizes the time which is necessary to propagate the wave packet from the region of the well where it is created up to the asymptotic region where it is absorbed by the optical potential. The large dispersion of the wave packet which exists at these two times then disappears under the action of the exponentially-decreasing terms and the wavefunction is finally projected on the single Floquet state $\lambda_{v=0, n=0}$ (see table 1). Nevertheless the large amplitudes of the non-diagonal elements of the matrices $\mathbf{R}(N, 1)$ and $\mathbf{R}(1, N)$ produce sufficiently large contributions during this lifetime to be observed in this non-adiabatic regime. In the adiabatic case, in contrast, each partial transition associated with $\mathbf{R}(i, i + 1)$ and $\mathbf{R}(i + 1, i)$ is too weak to be observed and disappears before the next can be created.

The imaginary part of the ‘pseudo-scattering’ states eigenvalues thus have a physical sense, even if (by contrast with the resonance eigenvalue $E_{\lambda_{v=0, n=0}}$) it is not an intrinsic sense. By displacing the optical potential in the direction of the inner well one observes an increase of the imaginary part of these ‘pseudo-scattering’ eigenvalues which takes into account the decreasing of the distance between the well and the absorbing region.

Finally, it is important to note that the ‘pseudo-scattering’ states do not contribute to the total dissociative flux. From the strict point of view of obtaining the total quantum flux at the completion of the experiment, the result obtained with a one-dimensional model space is correct (figure 11). The ‘pseudo-scattering’ states simply provide a correct time dependence of the dissociative wave packet and globally take into account the reaction time of the molecular system to the laser excitation.

4. Conclusion

The photodissociation of H_2^+ studied here confirms that the discrete version of the transport formula derived by Viennot *et al* [13, 14] is an efficient tool to describe such dynamical processes. The use of equation (9) in conjunction with a sequence of small active spaces

makes possible a large reduction of the CPU time in the case of long laser pulses with slowly varying envelopes. The origin of this benefit lies in the special discretization procedure used. By analogy with the difference between Riemann and Lebesgue integration, our approach uses a partition of the manifold of the adiabatic parameters (here the laser field amplitude $E(t)$) rather than a partition of the time, which is usual in integrating the Schrödinger equation.

The instantaneous Floquet eigenstates $|\lambda_{v,n}\rangle$ do not contribute equally to the sum appearing in equation (9). We should distinguish between the Floquet eigenstates issuing from the bound and the resonance eigenstates of $H_0 - iV_{\text{opt}}$ and those issuing from the states which discretize the molecular continua. The former constitute the framework of the process; they contribute directly to the dissociative flux and the imaginary part of their eigenvalues characterizes the dissociative flux which is transported by each eigenstate per unit time. The latter are introduced to describe the correct time dependence of the wave packet and of the associated dissociative quantum fluxes when the adiabatic parameters temporarily undergo fast variations. A few ‘pseudo-scattering’ states selected by the wave operator sorting algorithm to dress the eigenstates of the first group are generally sufficient to reproduce this behaviour correctly. The imaginary part of the eigenvalues characterizes the reaction time of the molecular system when it is subjected to a laser field.

The molecular system H_2^+ is elementary, principally because only one excited surface without structure is present. For a more complex system, many Floquet eigenstates issuing from the bound states and from the shape and Feshbach resonance states would be selected by the wave operator sorting algorithm. Nevertheless, we believe that the behaviour observed for H_2^+ would persist: each state of the first group would be dressed by a few Floquet eigenstates issuing from the ‘pseudo-scattering’ states to reproduce the temporary fast evolutions of the adiabatic parameters. The model space dimension would be larger for such bigger systems but would certainly remain negligible as compared with the full Hilbert space dimension.

References

- [1] Guérin S and Jauslin H R 2003 *Adv. Chem. Phys.* **125** 1–75
- [2] Dresse K and Holthaus M 1999 *Eur. Phys. J. D* **5** 119
- [3] Gravila M 2002 *J. Phys. B: At. Mol. Phys.* **35** R147
- [4] Berry M V 1990 *Proc. R. Soc. Lond. A* **429** 61
- [5] Jolicard G and Killingbeck J P 2003 *J. Phys. A: Math. Gen.* **36** R411–73
- [6] Fleischer A and Moiseyev N 2005 *Phys. Rev. A* **72** 032103
- [7] Breuer H P and Holthaus Z 1989 *Phys. D. At. Mol. Clusters* **11** 1
- [8] Peskin U and Moiseyev N 1993 *J. Chem. Phys.* **99** 4590
- [9] Guérin S 1997 *Phys. Rev. A* **56** 1458
- [10] Wyatt R E and Jung C 1997 *Mechanical studies of molecular spectra and dynamics Dynamics of Molecules and Chemical Reaction* ed R E Wyatt and J H Zhang (New York: Dekker)
- [11] Viennot D *et al* 2005 *Phys. Rev. A* **71** 052706
- [12] Aharanov Y and Anandan J 1987 *Phys. Rev. Lett.* **58** 1593
- [13] Viennot D, Jolicard G and Killingbeck J P 2006 *J. Phys. A: Math. Gen.* **39** 7065
- [14] Viennot D 2005 *Doctoral Thesis* <http://tel.ccsd.cnrs.fr/tel-00011145>
Viennot D, Jolicard G and Killingbeck J P Discrete evolutive active space in quantum dynamics (to be submitted)
- [15] Viennot D 2005 *J. Math. Phys.* **46** 072102
- [16] Bunkin F V and Tugov I I 1973 *Phys. Rev. A* **8** 601
- [17] Riss U V and Meyer H-D 1998 *J. Phys. B* **31** 2279
- [18] Riss U V and Meyer H-D 1995 *J. Phys. B* **28** 1475
- [19] Lefebvre R, Sindelka M and Moiseyev N 2005 *Phys. Rev. A* **72** 052704
- [20] Moiseyev N 1998 *J. Phys. B* **31** 1431
- [21] Jolicard G and Austin E J 1986 *Chem. Phys.* **103** 295
- [22] Jolicard G *et al* 2003 *J. Phys. B: At. Mol. Opt. Phys.* **36** 2777